ONLINE ACTIVITY MATCHING USING WIRELESS SENSOR NODES

Arie Horst and Nirvana Meratnia
Pervasive Systems, University of Twente, Drienerlolaan 5, Enschede, The Netherlands

Keywords: Activity matching, Body sensor network, Dynamic time warping.

Abstract: In this paper, we explore the capability of wireless sensor networks to perform online activity matching for sport coaching applications. The goal is to design an algorithm to match movements of a trainee and a trainer online and to find their spatial and temporal differences. Such an algorithm can aid the trainer to better observe performance of the trainees in group lessons.
We consider fitness-like movements such as those performed in aerobic. We also limit ourselves to only having one sensor node on the trainer and one sensor node on the trainee, however our algorithm scales well to more trainees per trainer. We use Sun SPOT sensor nodes and use the accelerometer and gyroscope sensors to capture the movements. The gravity vector is extracted and improved with a Kalman filter using the accelerometer and gyroscope data. An automatic segmentation technique is developed that examines the movement data for rest and activity periods and changes in movement direction. The segmentation and the movement information are communicated with the node of the trainee where the movements are compared. We choose to use Dynamic Time Warping (DTW) to perform the spatial and temporal matching of movements. Because DTW is computationally intensive, we develop an optimized technique and provide feedback to the trainee. We test all the design choices extensively using experiments and perform a system test using different test methods to validate our approach.

1 INTRODUCTION

A sport coach is a person who instructs and gives feedback to other individuals on correctness and their performance. The sport coach is often called a trainer and the individuals are often called trainees. Such a construction is very common in almost all sport domains, such as soccer, tennis, swimming, fitness, etc. In some of these domains the trainer has to instruct a group on how to perform a movement. Especially with large groups it becomes very difficult for the trainer to keep track of all the trainees and provide feedback to them. We try to address this problem by developing a system that assists the trainer with providing feedback to the trainees about correctness of their performance using a wireless sensor network.

A wireless sensor network (WSN) is a network of sensory devices that are wirelessly interconnected through a radio communication link. All these devices, also refered to as nodes, have some sort of processing unit to which sensors are attached and make perception of some physical quantity possible. Body sensor networks (BSN) are a special type of WSN in that they are mostly wireless but do not necessarily need to realize this via a radio link. BSNs are comprised of nodes attached to a body and communicate with each other either via radio link, the host body or wires (Lo et al., 2005)(Jones et al., 2008).

Activity recognition is a field of research that investigates how to accurately detect different activities a person performs. Examples includes recognizing activities such as walking, sitting, standing, cooking and eating(van Kasteren and Krose, 2007)(Tran and Sorokin, 2008), recognizing gestures from video or motion sensor data (Whitehead and Fox, 2009)(Yin and Xie, 2007), or recognizing interaction between one or more persons or objects (Patterson et al., 2005)(Wu et al., 2007). The latter is also known as interaction detection.

Our work examines the use of BSNs to accomplish the task of finding spatial and temporal differences of human body motion between two persons using inertial sensors in an online and decentralized manner.

The remainder of this paper is organized as follows: First related work is discussed in section 2 after which a detailed description of the system architecture is given in section 3. The components of the ar-

Horst A. and Meratnia N..
ONLINE ACTIVITY MATCHING USING WIRELESS SENSOR NODES.
DOI: 10.5220/0003361100220031
In *Proceedings of the 1st International Conference on Pervasive and Embedded Computing and Communication Systems* (PECCS-2011), pages 22-31
ISBN: 978-989-8425-48-5

chitecture are described in more detail in section 4 to 6. Finally the evaluation and conclusion sections conclude this paper.

2 RELATED WORK

Activity recognition is a vast research domain that intersects with the domains of image processing, audio processing and motion sensor data processing.

A method for detection and classification of interaction between two persons is presented in the work of Ruzena Bajcsy et al. (Bajcsy et al., 2009). The goal of the system is to detect if a classified movement deviates from the normal case. To detect these situations a classification is made by selecting a feature which has ”minimum distance” to the feature that is tested. A similar method is used by Davrondzhon Gafurov et al. (Gafurov and Snekkenes, 2009) for gait recognition using wearable motion sensors. Sensors are placed on foot, hip, pocket and arm. The Euclidean distance of the feature vectors and a template is then compared with a specified threshold. Distance measures as used by Ruzena Bajcsy et al. (Bajcsy et al., 2009) and Davrondzhon Gafurov et al. (Gafurov and Snekkenes, 2009) are simple and generaly cheap in terms of computation. The main disadvantage of the method used by the authors is that it is not possible to detect timing related information.

Yuji Ohgi (OHGI, 2006) uses dynamic time warping (DTW) to analyse the motion of a swimmer's arm stroke and the swing of a golf club in an offline manner on a PC. DTW is a method for finding similarity in two timeseries that are not necessarily of the same length and speed and is mostly used in speech recognition. DTW can use any distance meaure to detect the similarity of two data sets. Furthermore, the two data sets do not need to be aligned. A disadvantage of DTW is that it is computationaly intensive.

Marin-Perianu et al. present a lightweight, inexpensive and fast incremental algorithm for calculating cross-correlation (Marin-Perianu et al., 2007). Using this method it is possible to calculate correlation coefficients on small resource constrained devices such as wireless sensor nodes. To validate the technique, an implementation is made that detects if two wireless sensor nodes move together or separately. The correlation function can detect similarity when the signals are shifted in time, but not when one signal is stretched. The optimization made by the authors to the correlation function introduces another disadvantage. Their method requires very accurate synchronization and cannot detect delays.

Jonathan Lester et al. propose a system that detects if two devices are carried by the same person (Lester et al., 2004). As a measure for similarity the coherence function is used which is a measure of similarity of two signals in the frequency domain. Using this technique they can successfully detect if two devices are carried by the same person with detection rates up to 100%, even when the system is fooled by two persons walking in step. By using frequency domain signals, all timing information is lost and therefore, detecting delays is not possible. Additionaly, a time stretched signal will have very different frequency characteristics than the orignal signal.

3 SYSTEM ARCHITECTURE

In this section a top-down explanation of our system architecture is given. Nodes placed on the trainer are designed as Master and the nodes placed on the trainee are designed as Slave. Furthermore, the mapping of the master nodes to the slave nodes is one-to-one. This means that if a master node is placed on the left wrist, the slave node should also be placed on the left wrist and exchange of sample data happens only between these two nodes. This is defined as a *pair of nodes*. More than one slave can be connected to a master but we will not consider this case. Figure 1 shows an example of two pairs of nodes placed on the trainer and the trainee. We choose to place the sensors on the wrist because at the wrist high accelerations can be measured, while the sensor can still be attached without causing much discomfort.

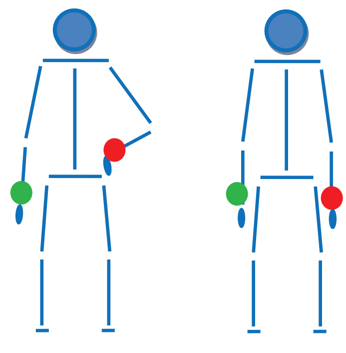

(a) Master (b) Slave

Figure 1: Sensor Placement.

The sensor hardware used are the PY530A gyroscope and the build-in LIS3L02AQ accelerometer of the Sun Spot nodes.

Taking the level one step lower to the software level the following components are required on the nodes, of which some are master or slave specific.

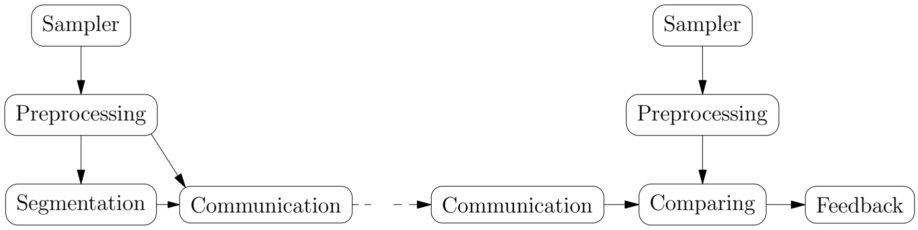

(a) Master (b) Slave

Figure 2: Software components.

The software components of our system architecture are shown in Figure 2.

Sampling is the process of taking data samples of the sensors. This component is subject to strict and accurate timing as subsequent processing may fail otherwise. This component is needed on both master and slave.

Preprocessing involves conditioning and refining the sensor data and extracting features from the sensor data. This is done in the preprocessing component which will be elaborated in section 4.

Segmentation is used to mark the beginning, change and end of movements in the sensor data stream. The segmentation component runs only on the master node as the trainer is supposed to do it right. The methods used to accomplish the segmentation are explained in section 5.

Communication between the master and the slave node is done wirelessly using the wireless communication capability of the sensor node.

Comparing of movement data is done on the slave nodes. The comparison identifies differences in the amplitude, direction, and timing of movements. The algorithm used for this process is further elaborated in section 6.

Feedback is generated from the result of the comparison of movement data and is sent to the base station.

4 PREPROCESSING

In the preprocessing stage, we filter out noise and extract the gravity vector from the accelerometer data.

To cancel out noise, a technique called oversampling (Watkinson, 1993) can be used. Noise tends to have the highest concentrations near the sampling frequency because aliases of all higher frequency noise will show up there. By oversampling this noise is moved away from the measured frequency band. The highest frequency of movements is emperically found to be 10Hz. According to the Nyquist theorem (Proakis and Manolakis, 2006), data should at least be sampled twice the time of the highest frequency component present in the measured signal. Therefore the sampling frequency should at least be 20Hz. Using oversampling we choose therefore to sample the sensor data at 40Hz.

The signal acquired from the accelerometer is the summation of the accelaration caused by gravity and the acceleration caused by movement of the device. This is an undersirable effect when comparing the movement directions, as how big the measured difference is then depends on the orientation of both devices.

We choose to extract the gravity vector from the signal of the accelerometer and then subtract this gravity signal from the accelerometer signal to obtain the movement vector. Having a movement vector with gravity eliminated allows better comparison of the movement direction.

A good first approximation of the gravity vector can be made using a low pass filter, but this approach may fail when the sum of the imposed acceleration and the gravity becomes very small. Here a kalman filter can help to make a better approximation of the gravity vector using the turn rates of the gyroscope.

To extract the gravity from the accelerometer data we choose to apply a low pass filter. A finite impluse response (FIR) filter is used because of its numerical stability (Proakis and Manolakis, 2006) and the fact that it is easy to implement. We have empirically found that, with regard to our specific type of considered movements, a cut-off frequency of 0.8Hz gives excellent results. The gravity vector from this filter is used as a basis and is further improved using a kalman filter and the rates of change from the gyroscope.

We choose to use a kalman filter to improve the estimation of the gravity vector with gyroscope data. This has the advantage of adding more speed when the orientation changes too quickly to be followed by the low pass filter. Also, the gravity extracted by the low pass filter suffers from overshoot, which will be damped by the kalman filter when the gyroscope data disagrees.

A kalman filter needs a model of the system to make an estimation of the new state of the system. The goal is to have a very lightweight kalman filter with respect to computational requirements. Others have used kalman filters like the unscented kalman filter in combination with quaternions to estimate orientation of a rigid body (Kraft, 2003) or a classic kalman filter with quaternions to estimate angular velocity and position (Yun et al., 2003). Saito H. et al. (Saito et al., 2009) use in their work a classic kalman filter to correct joint angles measured from gyroscope with inclination measured by an accelerometer.

We choose to use the Euler angles coordinate system so that a much smaller and simpler steady state kalman filter can be used. The advantage of a steady state kalman filter is that it is much more efficient from a computational demand point of view. The downside of using the Euler coordinate system is that it gives singularities at $\sim 90^\circ$. The alternative of a vector based model would require a rotation matrix as state transition matrix, which is time dependent. In that case only an extended kalman filter can be used to overcome the nonlinearity of the state transition matrix, which is computationaly too demanding.

5 SEGMENTATION

We have empirically found out that the algorithm to compare the movements needs specific periods of time to evaluate over. More specifically the best periods to evaluate are from a beginning to the end of a movement. To this end an algorithm is needed that makes a temporal segmentation of the real-time stream of data, such that each segment will hold at least one movement. This algorithm will run on the node of the trainer and will send segmentation events along with the stream of movement data to the node of the trainee.

Segmentation techniques can be classified in manual segmentation (Jafari et al., 2007) and automatic segmentation (Guenterberg et al., 2007)(Guenterberg et al., 2009)(Chambers et al., 2004). Manual segmentation can be done offline by examining the data or online using for example a pushbutton. Both of them are regarded as unacceptable as both the trainee and the trainer should not be concerned with such a task and offline segmentation is just not possible as the entire system is to run online in real-time. Guenterberg et al. (Guenterberg et al., 2007) present an automatic segmentation technique using windowed standard deviation to detect transitions between sitting and standing states of a human body. Another algorithm also from Guenterberg et al. uses the signal energy to distinguish between rest and activity states (Guenterberg et al., 2009). Chambers et al. (Chambers et al., 2004) calculate the log likelihood function over a sliding window. Sharp changes of the likelihood values correspond to change of acceleration value. Others have used the most simple form of segmentation by using a sliding window with some overlap (Patel et al., 2009).

All mentioned automatic segmentation techniques suffer from the problem that stationary signals are detected as rest. As the movements considered in our scenario can be relatively slow, these methods are not usable.

Instead we use two separate methods to detect segmentation points. The first method detects whether the node is moving, and the second method detects changes in movement direction. The results of these two methods are then combined to generate segmentation events that will be sent to the slave.

The first method we use takes the magnitude of the movement vector and the absolute value of the rates of change of the gyroscope to detect activity or rest. Three windowed moving average filters, one for the movement magnitude data and two for the gyroscope data, are used to smoothen the signals. When at least one of these moving averages becomes higher than a certain threshold, the node is considered moving. When all the averages are lower than a certain threshold, the node is considered not moving. A hysteresis between these two thresholds is applied to prevent oscillation of the movement state.

The second method we use detects abrupt changes in movement direction. This method evaluates the dot product of the current movement direction with a number of movements from recent history, as specified by Equation 1.

$$f(i,m,n) = \sum_{j=m}^{n} 1 - \vec{x}_i \cdot \vec{x}_{i-j} \qquad m > 0 \quad n > m \quad |\vec{x}_i|, |\vec{x}_{i-j}| > 0.2 \tag{1}$$

The input vector $\vec{x}$ must be normalized so that the dot product produces the cosine of the angle. The result of the dot product is then inverted such that two vectors pointing at the same direction produce zero and two vectors pointing at opposite direction produce two. This is evaluated and summed for a number of vectors from recent history starting at $i-m$ till $i-n$ such that the result is smoother. We have empirically found that the magnitude of the vectors (unnormalized) should be bigger than 0.2 to prevent noise triggering the algorithm.

We choose to use a threshold to generate a direction change event that will be used by the fusion algorithm that will fuse the results of the two methods.

This direction change event is generated only when Equation 1 becomes higher than a certain threshold.

The two methods are fused using the movement state and the direction change event. When the state of movement transits from rest to moving a "Movement Start" segmentation event is generated. A "Movement Stop" event is generated when the state of movement transits from moving to rest. When the movement state is moving, events from the direction change detection are allowed. In principle both event types can occur with quick succession. This is prevented by allowing events to occur only when a timeout has expired since the last event.

6 COMPARING MOVEMENTS

The measurements of the sensors are a representation of the movements made by the person to which the sensor node is attached. These measurements are then transfered from the node of the trainer to the node of the trainee, where they are compared to find differences in their movements.

There are many methods to accomplish this, such as the work of Ryan Aylward et al. (Aylward, 2006) and Martin Wirz et al. (Wirz et al., 2009) who use correlation as a measure of similarity of movements. The standard correlation function is improved by making it incremental by Marin-Perianu et al. in (Marin-Perianu et al., 2007), who also successfully used it to measure similarity. Another method is used by Jonathan Lester et al. (Lester et al., 2004) who used Coherence to measure similarity.

What all these methods have in common is that they produce poor results when movements are very similar and differ only in speed. We choose therefore the similarity measure used by Yuji Ohgi (OHGI, 2006), in which dynamic time warping (DTW) is used to assess the performance of swimmers and golfers. DTW in its classic form as used by Ohgi is however not suitable to be used in an online and realtime manner.

To overcome this problem we present an optimized version of the classic DTW in terms of computational requirements. Our new technique, fast incremental dynamic time warping (FIDTW), computes the optimal shortest warping path and can run on low power and resource constraint devices. Firstly, we provide some background on DTW with a mathematical definition and some notes on related work regarding optimization of the conventional DTW algorithm. The remainder of this section will be devoted to the optimization of the DTW algorithm and we finish with an evaluation of the choosen algorithm.

6.1 Classic DTW

DTW is a general time alignment and similarity measure for two temporal sequences and was first introduced by Bellman (Bellman, 2003). Suppose we have the sequences $C(i), 1 \le i \le l, C(i) \in R$ and $T(j), 1 \le i \le l, T(j) \in R$. These are called a class sequence and a test sequence, respectively. With these two sequences an $I \times J$ distance table $D(i,j)$ is constructed with which similarity can be measured. From the distance table a warping path W is then calculated which consists of a set of table elements that defines a mapping and an alignment between $C(i)$ and $T(j)$.

$$W = \left\{ w(i(q), j(q)) \;\middle|\; \begin{array}{l} q = 1, \ldots, Q \\ max(i,j) \le Q \le I + J - 1 \end{array} \right\}$$

where $i(q) \in \{1, \ldots, I\}$ and $j(q) \in \{1, \ldots, J\}$.

This warping path is restricted by *Continuity*, *Monotonicity* and *Endpoint* (the path must start at $i(1) = 1,\ j(1) = 1$ and end at $i(Q) = I,\ j(Q) = J$). By summing the local distances over the warping path, the local distance $DTW(C,T)$ is obtained. One of the possible choices for finding the best alignment between the two sequences is to find the warping path with the minimum DTW distance out of all possible warping paths. With the following recursive steps, the optimal warping path can be found and applies local constraints to the path:

$$D(i,j) = d(i,j) + min \left\{ \begin{array}{l} D(i-1, j-1) \\ D(i, j-1) \\ D(i-1.j) \end{array} \right\}$$

The recursion is generally initialized as $D(1,1) = d(1,1)$ and terminates when $i = I$ and $j = J$. The time and space complexity of this approach is $O(IJ)$.

6.2 Fast Incremental Dynamic Time Warping Algorithm

In this section we explain our optimization made to the classic DTW algorithm. One should first note that the aim of the optimization is to make it faster in terms of required computation time and not necessarily make it less resource hungry in terms of required memory space. Secondly the optimization should preserve all the characteristics of the classic DTW, which means that:

- The optimal warping distance should be preserved.
- The optimal warping path should be preserved.
- The optimal warping path must be able to be reconstructed afterwards for analysis.

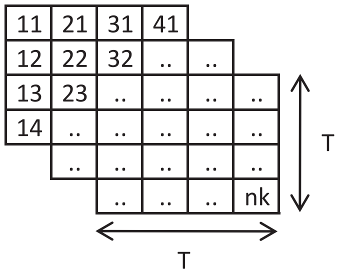

(a) Reshaped DTW

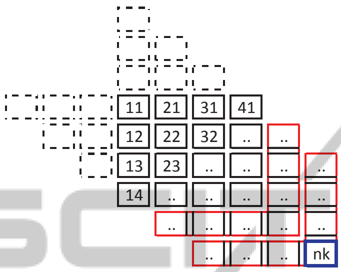

(b) Appearing stacked arrow form

Figure 3: Optimization steps of DTW.

Additionally, the algorithm should work with two real-time streams that are expected to be synchronized in time with an negligible error. In case of time synchronized data, it is also observed that:

- The diagonal line from top-left to bottom-right represents one-to-one allignment of time.
- A warping path that deviates from the diagonal to the lower left side means that sequence 1 has a delay compared to sequence 2.
- A warping path that deviates from the diagonal to the upper right side means that sequence 2 has a delay compared to sequence 1.

When a maximum positive and negative delay T is considered, the DTW distance matrix can be reshaped as shown in Figure 3(a), where the lower left and upper right matrix elements that fall outside the delay T are removed. This is justified as the algorithm is required to be able to measure delays up to T. The now appearing shape takes the form of stacked arrows, as can be seen in Figure 3(b). This arrow shape is from here on called an *arrow object* and all the elements enclosed by the arrow shape *directly belong* to the arrow object. The element of the arrow object which is emphesized by a blue box is from here on called the *center* of the arrow object. The stack form will be exploited to make the algorithm incremental. The main construct of the algorithm will then be a list of these arrow objects. The list is extended at the head until a maximum length L, after which one arrow object is removed from the tail everytime an arrow object is added at the head.

In classic DTW, the accumulated distance matrix is recomputed everytime the first row or column is removed. One reason for this is because otherwise the path distance obtained from the accumulated distance matrix will not be representative anymore. Also from a practical point of view when dealing with stream data, values cannot be added into infinity. One possible way of dealing with this is to recalculate the accumulated distance matrix when needed, but this would still has $\sim O(n^2)$ computation time.

It is observed from the classic DTW algorithm that due to local constraints, only immediate neighbour information is needed to calculate the accumulated distance at a certain point in the matrix. This means that when a new arrow object is added, the accumulated distances of this new arrow need only to be consistent with its successor. However, the accumulated distances are also used to find the shortest DTW path by traversing backward through the accumulated distance matrix. This is solved by immediately storing the neigbor with the lowest accumulated distance for all the elements of the new arrow object, so that the shortest DTW path can be found without the accumulated distances. Now that the accumulated distances of the new arrow object are calculated and the reason to keep the accumulated distances consistent is eliminated, the accumulated distances of the new arrow object can safely be adjusted. The only valid method for adjustment is subtraction, because division would cause range inconsistency of the distances of a new arrow object with the accumulated distances of its successor.

Although it is justified to make the adjustment by subtracting the lowest accumulated distance in the arrow object, only one-eight of the lowest accumulated distance is subtracted to better preserve the scale that these distances represent. This is required for the Flexible Endpoint algorithm that will be explained in section 6.2.1.

To derive the computational complexity of adding a new arrow object we assume one penalty for computing the distance of an element and three penalties for computing the accumulated distance of an element. This needs to be computed for T elements of an arrow object (see Figure 3(b)) so that the total computational complexity becomes $\sim O(6T)$. There is no penalty for computing the neighbour with lowest accumulated distance because this is already computed when the accumulated distance of an element is calculated, and requires only extra storage per element of an arrow object. However, traversing backwards along the warping path becomes slightly faster. The distance of a warping path is now obtained by adding up all the distances when traversing backward along the warping path, as the elements of the accumulated distance matrix do not represent real distances anymore.

6.2.1 Flexible Endpoint

While testing the algorithm, we found out that the algorithm may find a warping path with a very high distance although the two signals were very similar but slightly delayed. An example of such a case is shown in Figure 4(a). From this figure it can be seen that the distance in the area at the bottom right corner is very large. This is because the movement of the trainer is finished at this point, but the trainee did not. From Figure 4(a) it can be seen that there is an area with very high distances at the bottom right corner. The DTW path has to cross this area to reach the bottom right corner, which gives the wrong impression that the two movements are very distant.

This problem is solved by allowing flexible endpoint at the start of the path at the bottom right corner. The bottom right corner is the head of the list of arrow objects of the FIDTW algorithm. Evaluation of the shortest DTW path starts at the head of the list of arrow objects at the center of the arrow (the blue box in Figure 3(b)). A flexible endpoint algorithm therefore finds a more suitable start position in this arrow object. Flexible endpoint algorithms are widely used with DTW. It is unclear who first proposed the use of flexible endpoints, but probably one of the first to propose such a technique is Haltsonen (Haltsonen, 1985).

We choose to accomplish the task by taking the accumulated distance of the center of the arrow object as reference and find an accumulated distance in the arrow that is at least 25% or lower than the reference with a 1% penalty for every element it is further away from the reference. An example of a path produced with the flexible endpoint algorithm is shown in Figure 4(b). The path is identical, except in the bottom right corner, where the path produced with the flexible endpoint approach does not end in the far bottom right corner.

6.2.2 Distance Calculation

The distances for the DTW distance matrix are a combination of distance measures of multiple sources. The used sources are the magnitude of the movement, the direction of the movement and the change of orientation as measured by the gyroscope. The distance between the movement magnitudes are calculated using the squared Euclidean distance function (Equation 2). A magnitude is only one value such that equation

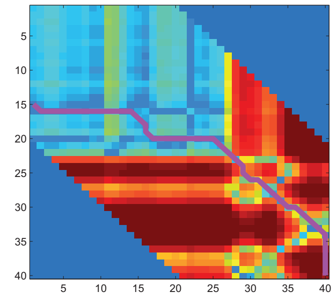

(a) Classic DTW path

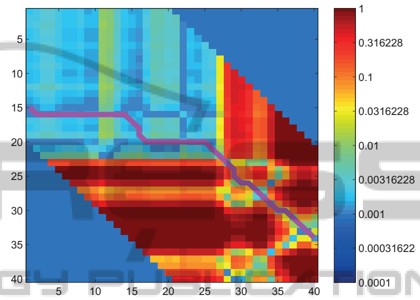

(b) Flexible endpoint

Figure 4: DTW paths.

2 simplifies to Equation 3

$$d(p,q) = \sum_{i=1}^{n} (p_i - q_i)^2 \qquad (2)$$

$$d(p,q) = (p-q)^2 \qquad (3)$$

The changes of orientation measured by the gyroscope are linear, therefore the Euclidean distance can safely be used as a distance measure. For a two dimensional gyroscope n becomes 2 in Equation 2.

The distance between the direction of movements is measured using Equation 4, which calculates the angle between two vectors by evaulating the arc cosine of the dot product of the two normalized movement vectors. This distance measure is only evaluated when the magnitude of both vectors is large enough, because the noise becomes more dominant when the magnitude of the movement is small.

$$d(\vec{x}_1, \vec{y}_1) = \arccos(\vec{x}_1 \cdot \vec{y}_1) \quad |\vec{x}_1|, |\vec{y}_1| > 0.2 \qquad (4)$$

These three distances are then combined by multiplying them with a weight factor and then adding them up to one distance measure (Equation 5). The weight factors facilitate the calibration of the system.

$$\begin{aligned} d_{combined} = W_{magn} * d_{magn} + \\ W_{dir} * d_{dir} + W_{orient} * d_{orient} \end{aligned} \qquad (5)$$

6.3 Path Analysis

With the temporal segmentation information an analysis of the path produced by the FIDTW algorithm can be made. From this analysis appropiate feedback can be given to the trainee. From the DTW path a number of statistical data can be extracted. Figure 5 depicts a typical path produced by our FIDTW algorithm when two movements are very similar. The diagonal elements from bottom-right to top-left of the distance matrix represent perfect time alignment. With respect to the stated direction of the diagonal line, a deviation to the right represents a positive delay and deviation to the left represents a negative delay. Small differences between two movements may already cause small delays, often shifting back and forth from positive to negative delays. Therefore we use the mean of the delays in a segment.

The DTW path distance represents the similarity of two signals. This distance also depends on the length of the path and is therefore normalized by the path length. The smaller the path distance the more similar the movements are.

When the path distance is high the two movements are detected as dissimilar. The cause of the high distance needs to be found. This information is, for every element, stored in the DTW distance matrix. Then during path analysis this information is recovered from the distance matrix such that it can be used as feedback.

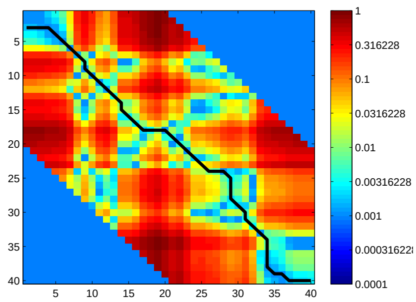

Figure 5: Example DTW path.

7 EVALUATION

We assess the correctness of our online matching technique using three different methods:

1. The node of the trainer and the node of the trainee are both placed on the same wrist of one person. This test should always label the movements as correct and not delayed.
2. The node of the trainer is placed on one wrist and the node of the trainer on the other wrist of one person. With this test there is already no real ground truth anymore, other than the feeling of the person that he made the same movement with both arms.
3. One person wears the master node on the right wrist while another person wears the slave node on the right wrist.

The feedback which is sent from the slave node holds information about the incorrectness of the movement, the timing and the cause of the incorrectness. The measure for incorrectness is the distance between the movements measured using the FIDTW algorithm. The timing is either an earlyness or a lateness in the form of a positive or negative average delay. When the distance is larger than a certain threshold, the movement can be regarded as incorrect.

7.1 Test Methodology

For the three test methods a test set of three tests, mentioned in Table 1, is defined. This test set consists of repetitive distinct movements. For every test in the set there is one movement repetition defined for the master node and multiple variations of this movement for the slave node. These variations differ in direction, in amplitude and in timing.

Table 1: Test set.

Test	Description
1	Stretched arm swings 90 degrees from horizontal to vertical position in the upward direction and goes back to the horizontal position.
2	Right arm is stretched away from the body to the right in a horizontal straight line and then attracted to the body again.
3	Right arm is stretched away from the body in the upward direction in a vertical straight line and moves back towards the body again.

7.2 Summary of Results

All tests are made indoors in a room with good radio reception to prevent link losses corrupting the measurements. For method 1 all tests are repeated three times, and for methods 2 and 3 the tests are repeated two times. The duration of every test is about 20 seconds, during which the movement is repeated continuously without rest. This results in about ten repeated identical movements, which should be detected and classified by the algorithm. The classification can be either correct or incorrect. The correct classification rate then is the number of correctly classified movements over the total number of movements presented in percentage for each method of testing.

In the tests with method 1 the master and slave nodes are both attached to the same wrist of the performer. Therefore, there are no variations for the slave node and the expected result is that the algorithm classifies all the movements as identical. We repeated all tests three times and obtained a correct detection rate of 99%.

In the tests with method 2 the master and slave nodes are attached to two wrists of one performer. Using clear differences in movements we asses if the algorithm correctly classifies the movements. The correct detection rate for identical movements, 45° direction difference, 90° direction difference, 0.5 second timing difference and 30cm distance difference are respectively 97%, 84%, 89%, 90% and 92%. We observed that direction differences are undetectable by the sensor nodes in this test. When the orientation of the sensor node would be known, this problem could be solved. However, obtaining an orientation is not easily accomplished.

In the tests with method 3 the master and slave nodes are attached to the right wrist of two performers. With this test we asses the real life performance of our algorithm. The correct detection rate for identical movements, 90° direction difference, 0.5 second timing difference and 30cm distance difference are respectively 86%, 83%, 60%, and 40%.

8 CONCLUSIONS AND FUTURE WORK

We presented an online and distributed activity matching algorithm using wireless sensor networks. Our experimental results show a high detection accuracy for identical movements, although it shows high sensitivity on how movements are performed

The most important open issue is to make the algorithm work reliably in detecting movement differences between two persons. The low reliability at present is partly caused by the orientation issue, but also because the algorithm is over sensitive to subtle movement differences. The solution to this problem may be found in using other distance measures and other sensors.

A second open issue is the orientation problem. Due to this problem, the sensor orientation must closely match when attached to the wrist, but also during movements the orientation must closely match. This makes testing with two persons hard and more unreliable. The problem maybe solved by using different sensors that allow to measure all degrees of freedom, such that the orientation can be derived. This is not an easy task and may not work reliably or fast enough to be used for this application.

The gravity detection may be further improved by using quaternions instead of euler angles, such that singularities are avoided. This will make the Kalman filter more complex, but will improve the reliability of the estimation.

Future work will also require an extensive evaluation with more users.

REFERENCES

Aylward, R. (2006). Sensemble: A wireless, compact, multi-user sensor system for interactive dance. In *Proc. of NIME 06*, pages 134–139.

Bajcsy, R., Borri, A., Benedetto, M. D. D., Giani, A., and Tomlin, C. (2009). Classification of physical interactions between two subjects. *Wearable and Implantable Body Sensor Networks, International Workshop on*, 0:187–192.

Bellman, R. E. (2003). *Dynamic Programming*. Dover Publications, Incorporated.

Chambers, G. S., Venkatesh, S., West, G. A. W., and Bui, H. H. (2004). Segmentation of intentional human gestures for sports video annotation. In *MMM '04: Proceedings of the 10th International Multimedia Modelling Conference*, page 124, Washington, DC, USA. IEEE Computer Society.

Gafurov, D. and Snekkenes, E. (2009). Gait recognition using wearable motion recording sensors. *EURASIP J. Adv. Signal Process*, 2009:1–16.

Guenterberg, E., Bajcsy, R., Ghasemezadeh, H., and Jafari, R. (2007). A segmentation technique based on standard deviation in body sensor networks. In *Dallas-EMBS '07: Proceedings of the IEEE Dallas Engineering in Medicine and Biology Workshop*. IEEE.

Guenterberg, E., Ostadabbas, S., Ghasemzadeh, H., and Jafari, R. (2009). An automatic segmentation technique in body sensor networks based on signal energy. In *BodyNets '09: Proceedings of the Fourth International Conference on Body Area Networks*, pages 1–7, ICST, Brussels, Belgium, Belgium. ICST (Institute for Computer Sciences, Social-Informatics and Telecommunications Engineering).

Haltsonen, S. (1985). Improved dynamic time warping methods for discrete utterance recognition. *Acoustics, Speech and Signal Processing, IEEE Transactions on*, 33(2):449 – 450.

Jafari, R., Li, W., Bajcsy, R., Glaser, S., and Sastry, S. (2007). Physical activity monitoring for assisted living at home. In *BSN '07: Proceedings of the 4th International Workshop on Wearable and Implantable Body Sensor Networks*, pages 213–219, Berlin, Heidelberg. Springer.

Jones, V., in 't Veld, R. H., Tonis, T., Bults, R., van, B. B., Widya, I., Vollenbroek-Hutten, M., and Hermens, H. (2008). Biosignal and context monitoring:

Distributed multimedia applications of body area networks in healthcare. In *Proceedings IEEE 10th Workshop on Multimedia Signal Processing, 2008*, pages 820–825, Cairns, Australia. IEEE Signal Processing Society.

Kraft, E. (2003). A quaternion-based unscented kalman filter for orientation tracking. In *Proceedings of the Sixth International Conference on Information Fusion*, volume 1, pages 47–54.

Lester, J., Hannaford, B., and Borriello, G. (2004). Are you with me? using accelerometers to determine if two devices are carried by the same person. In *In Proceedings of Second International Conference on Pervasive Computing (Pervasive 2004*, pages 33–50.

Lo, B. P. L., Thiemjarus, S., King, R., and zhong Yang, G. (2005). Body sensor network - a wireless sensor platform for pervasive healthcare monitoring. In *Adjunct Proceedings of the 3rd International conference on Pervasive Computing (PERVASIVE'05*, pages 77–80.

Marin-Perianu, R., Marin-Perianu, M., Havinga, P., and Scholten, H. (2007). Movement-based group awareness with wireless sensor networks. In *PERVASIVE'07: Proceedings of the 5th international conference on Pervasive computing*, pages 298–315, Berlin, Heidelberg. Springer-Verlag.

OHGI, Y. (2006). Mems sensor application for the motion analysis in sports science. *ABCM Symposium Series in Mechatronics*, 2:501–508.

Patel, S., Mancinelli, C., Healey, J., Moy, M., and Bonato, P. (2009). Using wearable sensors to monitor physical activities of patients with copd: A comparison of classifier performance. *Wearable and Implantable Body Sensor Networks, International Workshop on*, 0:234–239.

Patterson, D. J., Fox, D., Kautz, H., and Philipose, M. (2005). Fine-grained activity recognition by aggregating abstract object usage. In *ISWC '05: Proceedings of the Ninth IEEE International Symposium on Wearable Computers*, pages 44–51, Washington, DC, USA. IEEE Computer Society.

Proakis, J. G. and Manolakis, D. G. (2006). *Digital Signal Processing Principles Algorithms and Applications*. Prentice hall (4th ed).

Saito, H., Watanabe, T., and Arifin, A. (2009). Ankle and knee joint angle measurements during gait with wearable sensor system for rehabilitation. In *World Congress on Medical Physics and Biomedical Engineering*, pages 506–509, Berlin, Heidelberg. Springer.

Tran, D. and Sorokin, A. (2008). Human activity recognition with metric learning. In *ECCV '08: Proceedings of the 10th European Conference on Computer Vision*, pages 548–561, Berlin, Heidelberg. Springer-Verlag.

van Kasteren, T. and Krose, B. (2007). Bayesian activity recognition in residence for elders. In *Intelligent Environments, 2007. IE 07. 3rd IET International Conference on*, pages 209–212.

Watkinson, J. (1993). *The Art of Digital Audio*. Butterworth-Heinemann, Newton, MA, USA, 2nd edition.

Whitehead, A. and Fox, K. (2009). Device agnostic 3d gesture recognition using hidden markov models. In *Future Play '09: Proceedings of the 2009 Conference on Future Play on @ GDC Canada*, pages 29–30, New York, NY, USA. ACM.

Wirz, M., Roggen, D., and Troster, G. (2009). Decentralized detection of group formations from wearable acceleration sensors. *Computational Science and Engineering, IEEE International Conference on*, 4:952–959.

Wu, J., Osuntogun, A., Choudhury, T., Philipose, M., and Rehg, J. M. (2007). A scalable approach to activity recognition based on object use. In *In Proceedings of the International Conference on Computer Vision (ICCV), Rio de*.

Yin, X. and Xie, M. (2007). Finger identification and hand posture recognition for human-robot interaction. *Image and Vision Computing*, 25(8):1291 – 1300.

Yun, X., Lizarraga, M., Bachmann, E., and McGhee, R. (2003). An improved quaternion-based kalman filter for real-time tracking of rigid body orientation. In *Intelligent Robots and Systems, 2003. (IROS 2003). Proceedings. 2003 IEEE/RSJ International Conference on*, volume 2, pages 1074–1079.